

## Article

# Novel Technology for Comprehensive Utilization of Low-Grade Iron Ore

Xinran Zhu <sup>1,2,\*</sup>, Yonghong Qin <sup>1,2</sup>, Yuexin Han <sup>1,2</sup> and Yanjun Li <sup>1,2</sup>

<sup>1</sup> College of Resources and Civil Engineering, Northeastern University, Shenyang 110819, China; qyh\_neu@163.com (Y.Q.); dongdafulong@mail.neu.edu.cn (Y.H.); liyanjun@mail.neu.edu.cn (Y.L.)

<sup>2</sup> National-Local Joint Engineering Research Center of High-Efficient Exploitation Technology for Refractory Iron Ore Resources, Shenyang 110819, China

\* Correspondence: zhuxinran@mail.neu.edu.cn; Tel.: +86-24-8368-7120; Fax: +86-24-8368-8920

**Abstract:** In this study, a novel technology for the comprehensive utilization of low-grade iron ore is presented. For the iron ore with a Fe content of 24.91%, a pilot-scale study of pre-concentration, suspension magnetization roasting, grinding, and low-intensity magnetic separation was conducted, and an iron concentrate with a grade of 62.21% and a recovery of 85.72% was obtained. The products were analysed using chemical elemental analysis, particle size analysis, X-ray diffraction, scanning electron microscopy, and vibrating sample magnetometry. The results indicated that hematite was reduced by CO and H<sub>2</sub> mixture and transformed into ferrimagnetic magnetite in the suspension magnetization roasting, which was easily recovered in the subsequent magnetic separation. Additionally, a pre-concentration tailing with a SiO<sub>2</sub> content of 81.55% and a magnetic tailing of the roasted ore with a SiO<sub>2</sub> content of 79.57% were obtained, which can be used as building materials. This presents significant implications for the comprehensive utilization of low-grade iron ore.

**Keywords:** hematite; quartz; iron concentrate; building material; suspension magnetization roasting



**Citation:** Zhu, X.; Qin, Y.; Han, Y.; Li, Y. Novel Technology for Comprehensive Utilization of Low-Grade Iron Ore. *Minerals* **2022**, *12*, 493. <https://doi.org/10.3390/min12040493>

Academic Editor: Jakub Kierczak

Received: 1 April 2022

Accepted: 14 April 2022

Published: 18 April 2022

**Publisher's Note:** MDPI stays neutral with regard to jurisdictional claims in published maps and institutional affiliations.



**Copyright:** © 2022 by the authors. Licensee MDPI, Basel, Switzerland. This article is an open access article distributed under the terms and conditions of the Creative Commons Attribution (CC BY) license (<https://creativecommons.org/licenses/by/4.0/>).

## 1. Introduction

As the most consumed basic structural and functional materials, steel plays an irreplaceable role in the development of the national economy, national security, and people's life [1]. With the rapid development of the economy and society of China, the requirement for iron and steel will remain at a high level for quite a long time in the future [2,3]. However, the iron and steel industry of China has been facing a severe shortage of iron ore for a long time. That is to say, domestic iron ore cannot satisfy the demand of the iron and steel industry in China [4]. At present, the iron and steel industry of China relies heavily on the iron ore imported from Australia and Brazil, which has affected the stable operation of the iron and steel industry [5].

China has abundant iron ore resources and the reserve is 85.22 billion tons [6]. However, the majority consists of low-grade iron ore with complex mineral composition and fine dissemination [7]. Currently, the average grade of iron ore in China is approximately 30%, and more than 90% of the iron ore needs processing before being used in the iron and steel industry [8]. Therefore, the utilization of low-grade iron ore resources is conducive to lessening the dependence on imported iron ore resources, which also has significance for the exploitation of low-grade iron ore globally.

The effective and economical beneficiation of low-grade hematite ore is an acceptable technical problem due to the low iron grade, complex mineral composition, and fine dissemination [9]. A large amount of research has been conducted to process low-grade hematite ore in recent years [10–12]. The typical processing methods include gravity concentration [13,14], magnetic separation [15,16], froth flotation [17–19], and their combinations such as low-intensity magnetic separation–high-intensity magnetic separation–reverse flotation, magnetic separation–gravity separation–reverse flotation, and stage-

grinding–classification–gravity separation–anion reverse flotation [20–22]. Although the production index has improved based on these processes, it still faces the issues of complex processing routes and poor adaptability to the variation of raw ore. In addition, large amounts of tailings were produced in the beneficiation process of low-grade iron ore, which has caused severe environmental problems, such as land occupation, reclamation, and water pollution [23–25]. Thus, it is essential to develop novel technologies to achieve the comprehensive utilization of low-grade iron ore resources.

Magnetization roasting is an effective method to process hematite ore, in which hematite is reduced to magnetite and easily recovered by low-intensity magnetic separation [26,27]. Currently, with the development of magnetization roasting technology and associated industrial equipment, suspension magnetization roasting technology has become a promising method for processing low-grade hematite ore [28–30]. It has the advantages of a low roasting temperature, a large production capacity, and a simple process route [31]. Additionally, owing to the destruction of the ecological environment associated with sand mining, the exploitation of river sand and gravel has been limited by the government, which has caused market fluctuations in the construction industry [32,33]. The requirement of alternative building materials has brought a good opportunity for the comprehensive development and utilization of tailings resources [34–38]. According to Yellishetty et al. [39], iron ore mineral waste can be used in concrete, construction, and bricks due to particle sizes. Xu et al. [40] recycled kaolin tailing sand (KTS) as an eco-friendly alternative for natural river sand as a fine aggregate in producing cement mortar and concrete, finding that the mechanical performance was best with 60 wt.% KTS replacement. Vargas et al. [41] calculated the environmental impacts of the use of copper treated tailings (TT) as supplementary cementitious materials, indicating the TT mixtures showed better environmental indicators at a higher mechanical performance. Loginova et al. [42] found that the municipal solid waste incineration bottom ash was a potential minor additional constituent for cement.

In this study, a novel technology for the comprehensive utilization of low-grade iron ore is presented. In this process, the samples were analysed using chemical elemental analysis, X-ray diffraction (XRD), vibrating sample magnetometry (VSM), and scanning electron microscope (SEM). The phase transformation, magnetism variation, and micromorphology were characterized in suspension magnetization roasting (SMR). Moreover, the elemental composition and particle size analyses of the tailings were conducted for their applications in building materials.

## 2. Materials and Experimental

### 2.1. Materials

The raw ore used in the experiment was obtained from opencast mining in Shanxi, China. It was crushed using a jaw crusher and a high-pressure roller mill, and the final particle size was below 1.5 mm. The chemical elemental analysis of the raw ore is shown in Table 1. It is indicated that the Fe content was 24.91% and the FeO content was 2.75%, which was attributed to the presence of small amounts of magnetite and siderite. The primary gangue mineral was quartz and the SiO<sub>2</sub> content was 46.90%. Other impurities were MgO (0.95%), Al<sub>2</sub>O<sub>3</sub> (2.02%), and CaO (2.13%). The contents of harmful elements P and S were 0.047% and 0.072%. Based on the XRD results (Figure 1), the primary iron minerals of the raw ore were hematite, magnetite, and siderite. The gangue minerals were quartz, carbonates, etc.

**Table 1.** Chemical elemental analysis of raw ore.

Composition	Fe	FeO	SiO <sub>2</sub>	MgO	Al <sub>2</sub> O <sub>3</sub>	CaO	P	S
Content (wt.%)	24.91	2.75	46.90	0.95	2.02	2.13	0.047	0.072

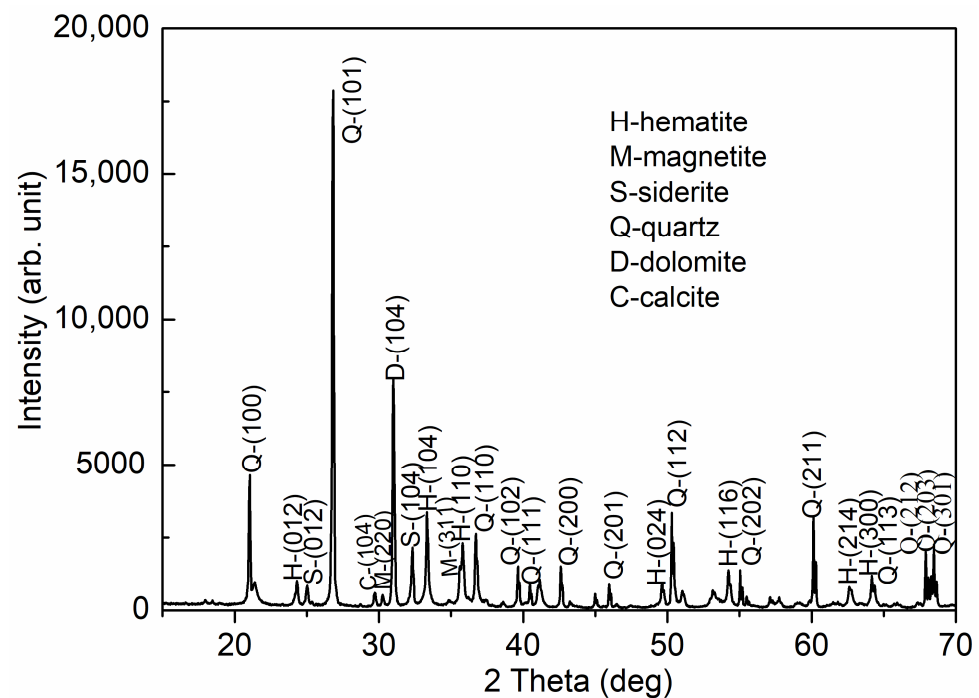


Figure 1. XRD analysis of raw ore.

## 2.2. Experimental Equipment and Methods

A schematic diagram of the comprehensive utilization of the low-grade iron ore is shown in Figure 2. It was mainly composed of pre-concentration, suspension magnetization roasting, and magnetic separation. The raw ore was ground using a ball mill, and the particle size was 60 wt.% passing 0.075 mm. Then, the ground product was processed using three-stage magnetic separation with the magnetic intensities of 143.31, 398.09, and 875.80 kA/m, respectively. The iron concentrate and tailing of the pre-concentration were obtained. The iron concentrate of pre-concentration was used as the feeding of suspension magnetization roasting. The suspension magnetization roasting system consisted of preheating, reduction, and cooling, in which antiferromagnetic hematite transformed into ferrimagnetic magnetite. The reducing agent was composed of CO and H<sub>2</sub> with a volume ratio of 2:1. The roasted ore was ground using a vertical stirring mill, and the particle size was 80 wt.% passing 0.038 mm. The ground product was processed using low-intensity magnetic separation with a magnetic intensity of 119.43 kA/m. Finally, the iron concentrate and magnetic tailing of the roasted ore were obtained.

## 2.3. Characterization

The chemical elemental analyses of raw ore and roasted ore were conducted. The Fe and FeO were determined using the chemical titration method. The SiO<sub>2</sub>, Al<sub>2</sub>O<sub>3</sub>, MgO, CaO, and P were determined using X-ray fluorescence (XRF) spectrometry (Primus II, Japan). The S was determined using a LECO SC-144DR sulfur analyzer (MI, USA). The raw ore and roasted products were analysed using an X-ray diffractometer (X'Pert PRO, PANalytical B.V., The Netherlands) at a scanning angle of 5–90° and a scanning speed of 12°/min. The magnetism properties of raw ore, pre-concentration concentrate, roasted ore, and iron concentrate were analysed using vibrating sample magnetometry (JDAW-2000D, Yingpu, China). The initial magnetization curves and hysteresis loops were analysed with magnetic field ranges of 0–637 and –637–637 kA/m, respectively. The roasted ore was analysed using scanning electron microscopy and an energy dispersive spectrum (ULTRA plus, Zeiss, Germany). Additionally, the micromorphology and elemental distribution were studied.

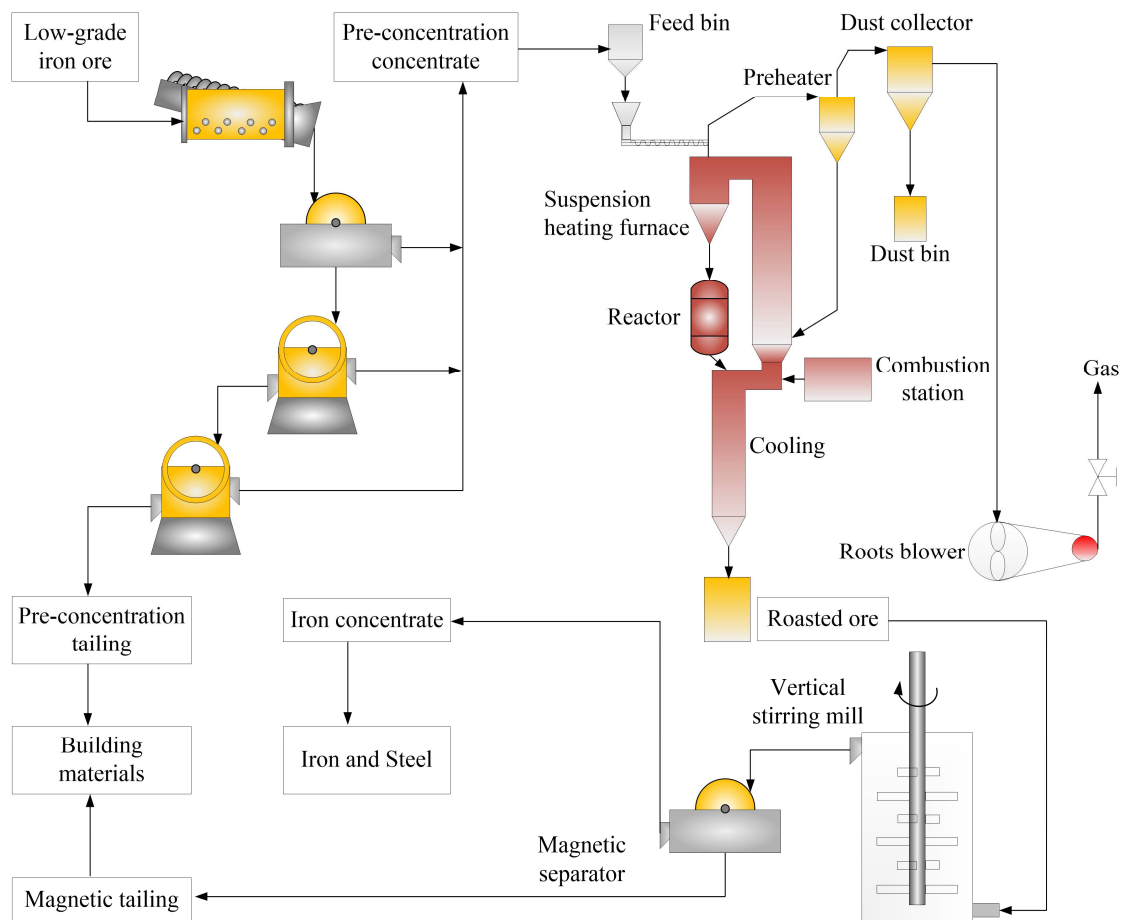


Figure 2. Schematic diagram of comprehensive utilization of low-grade iron ore.

### 3. Results and Discussion

#### 3.1. Pre-Concentration

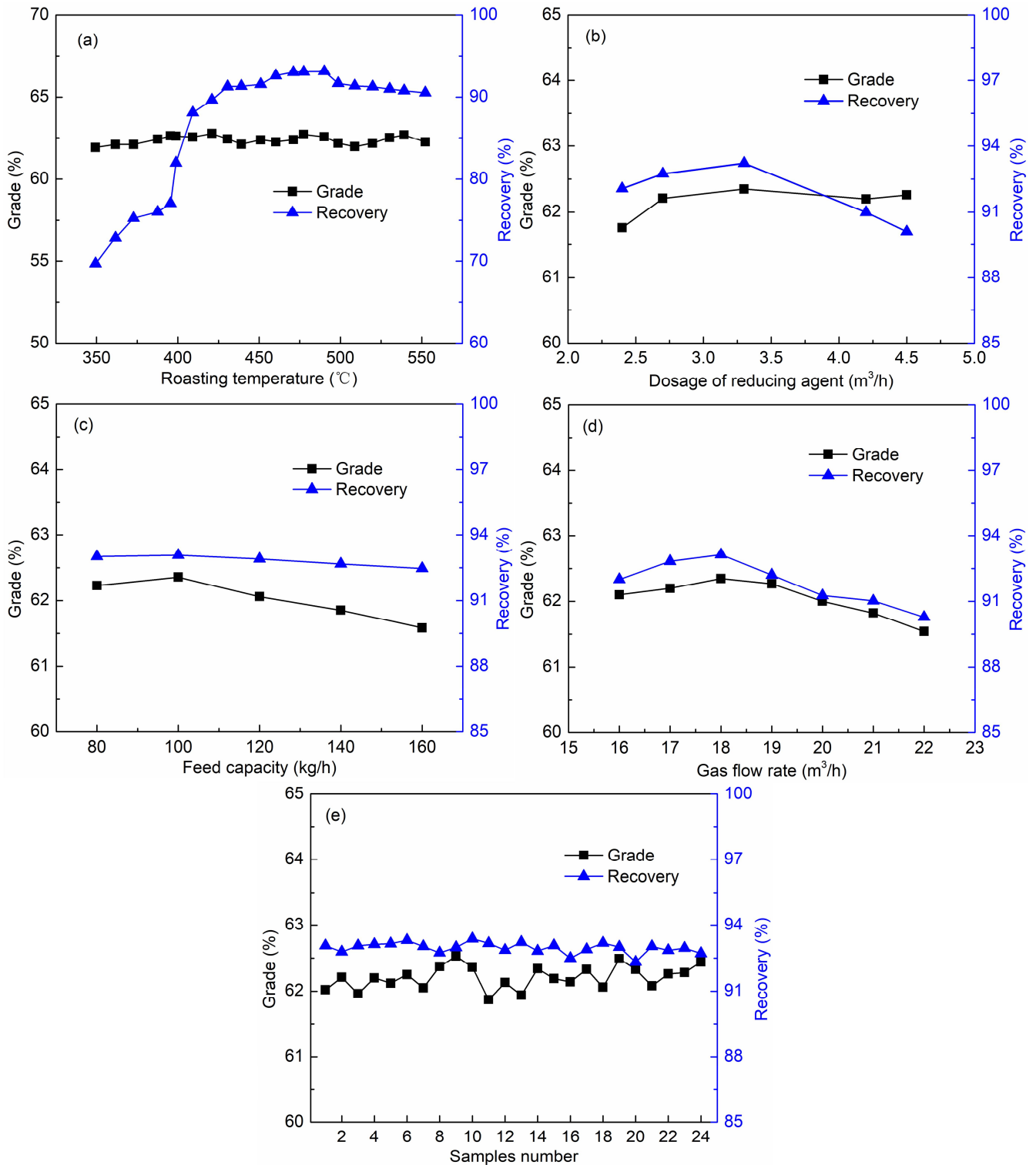
The raw ore was processed by a three-stage magnetic separation, and the separation indexes of pre-concentration concentrate and tailing are shown in Table 2. Based on the results, the tailing with a yield of 29.01% and an iron grade of 6.70% was removed before suspension magnetization roasting, which was conducive to lowering the roasting cost. In addition, the pre-concentration tailing with a SiO<sub>2</sub> content of 81.55% and an iron grade of 6.70% can be used for producing building materials. Finally, the pre-concentration concentrate with an iron grade of 32.35% and a recovery of 92.20% was obtained. Pre-concentration of low-grade iron ore could effectively remove some slime and gangue minerals and weaken their influence on the subsequent suspension magnetization roasting operation. Meanwhile, the processing capacity and efficiency have improved in suspension magnetization roasting.

Table 2. Separation index of low-grade iron ore in pre-concentration (wt.%).

Products	Yield	SiO <sub>2</sub> Grade	Fe Grade	Fe Recovery
Pre-concentration concentrate	70.99	32.74	32.35	92.20
Pre-concentration tailing	29.01	81.55	6.70	7.80

### 3.2. Suspension Magnetization Roasting

In this experiment, the effects of the roasting temperature of 350–550 °C, reducing agent dosage (CO:H<sub>2</sub> = 2:1) of 2.4–4.5 m<sup>3</sup>/h, feed capacity of 80–160 kg/h, and total gas volume of 15.0–22.0 m<sup>3</sup>/h on the magnetic separation index were studied, and the results are shown in Figure 3a–e.



**Figure 3.** Effects of roasting conditions on Fe grade and recovery of magnetic concentrate. (a) roasting temperature; (b) reducing agent dosage; (c) feeding capacity; (d) gas flow rate; (e) stable running test.

The iron grade and recovery of iron concentrate were the important indexes of the magnetization roasting effect. The iron concentrate grade  $\beta$  was obtained by the chemical element analysis, and the recovery  $\varphi$  was calculated by Equation (1) [8].

$$\varphi = \frac{\beta \cdot \gamma}{\alpha} \times 100\% \quad (1)$$

where  $\alpha$  is the Fe grade of the roasted ore,  $\beta$  is the Fe grade of the iron concentrate, and  $\gamma$  is the yield of iron concentrate.

### 3.2.1. Roasting Temperature

As shown in Figure 3a, with the increase in reduction temperature, the grade of magnetic concentrate fluctuated in the range of 61.91–62.76%, with an average value of 62.36%. The recovery of magnetic concentrate increased from 69.69% to 93.00% as reduction temperature increased from 349.4 to 471.1 °C. The recovery remained stable between 92.59% and 93.10% at a reduction temperature of 471.1–490.1 °C. When the roasting temperature exceeded 490 °C, the recovery of iron concentrate decreased gradually. This was because hematite was over-reduced to FeO at a high reduction temperature, resulting in a decrease in iron recovery in magnetic separation [31]. Therefore, iron concentrate with a grade of 62% and a recovery of 93% can be obtained at a reduction temperature of 471.1–490.1 °C.

### 3.2.2. Reductant Dosage

As shown in Figure 3b, when the reductant dosage was increased from 2.4 to 3.3 m<sup>3</sup>/h, the iron grade of concentrate increased from 61.76% to 62.35%, and the iron recovery increased from 92.07% to 93.22%. When reductant dosage varied from 3.3 to 4.5 m<sup>3</sup>/h, the iron grade of concentrate kept stable between 62.20% and 62.35%, while the iron recovery decreased from 93.22% to 90.10%. The result suggested that the appropriate reductant dosage was 2.7–3.3 m<sup>3</sup>/h. Hematite was over-reduced at the reductant dosage of 4.2–4.5 m<sup>3</sup>/h, resulting in a decrease in iron recovery. Thus, the appropriate reductant dosage was 3.3 m<sup>3</sup>/h, and an iron concentrate with an iron grade of 62.35% and a recovery of 93.22% was obtained.

### 3.2.3. Feeding Capacity

As shown in Figure 3c, the grade and recovery of iron concentrate tended to be stable at first and then decrease with the increase in feed capacity. When feed capacity increased from 80 to 100 kg/h, the grade of iron concentrate fluctuated in 62.23%–62.36%, and the iron recovery kept stable at approximately 93%. When the feed capacity increased from 100 to 160 kg/h, the grade of iron concentrate decreased from 62.36% to 61.58%, and the iron recovery decreased from 93.07% to 92.47%. This was because reducing time decreased with the increase in feeding capacity [8]. The appropriate feed capacity was determined as 100 kg/h.

### 3.2.4. Gas Flow Rate

As shown in Figure 3d, total gas volume had a significant impact on the grade and recovery of iron concentrate. When total gas volume increased from 16.0 to 19.0 m<sup>3</sup>/h, the grade of iron concentrate fluctuated between 62.10% and 62.35%, and the iron recovery peaked at 93.13% with a gas volume of 18.0 m<sup>3</sup>/h. As total gas volume continued to increase from 18.0 to 22.0 m<sup>3</sup>/h, the iron grade decreased from 62.27% to 61.54%, and the iron recovery decreased from 92.21% to 90.27%. We inferred that it hurt the roasting effect when total gas volume exceeded 18.0 m<sup>3</sup>/h [43]. Therefore, the appropriate total gas volume was determined as 18.0 m<sup>3</sup>/h.

### 3.2.5. Stable Running Test

To investigate the stability of equipment operation and production index, the stable running tests of suspension magnetization roasting were conducted at a feed capacity of

100 kg/h, a reduction temperature of 480 °C, a reductant dosage of 3.3 m<sup>3</sup>/h (CO:H<sub>2</sub> = 2:1), and a total gas volume of 18.0 m<sup>3</sup>/h. Based on the results (Figure 3e), an iron concentrate with an average grade of 62.21% and an average recovery of 92.97% was obtained. As the iron recovery of pre-concentration concentrate was 92.20%, the actual iron recovery corresponding to the raw ore was 85.72%.

### 3.3. Phase Transformation

To study the phase transformation in suspension magnetization roasting, the roasted samples at different roasting temperatures were analysed by XRD, and the results are shown in Figure 4. When the roasting temperature was 460 °C, the characteristic peaks of hematite vanished, while the characteristic peaks of magnetite appeared in the roasted ore, which was attributed to the transformation from hematite to magnetite as Equations (2) and (3). In addition, the characteristic peak 104 of siderite gradually weakened and disappeared at 500 °C owing to its thermal decomposition [44]. When the roasting temperature exceeded 520 °C, characteristic peaks 111 and 200 of wüstite (FeO) gradually presented, caused by the over-reduction of magnetite per Equations (4) and (5). Owing to the weak magnetism of wüstite, the generation of FeO lowered the iron recovery in the subsequent low-intensity magnetic separation. The phase transformation was consistent with the experimental results of roasting temperature in Figure 3a. Moreover, the gangue minerals of quartz and calcite did not change based on their characteristic peaks. The thermodynamics analysis of reduction reaction Equations (2)–(5) are shown in Figure 5.

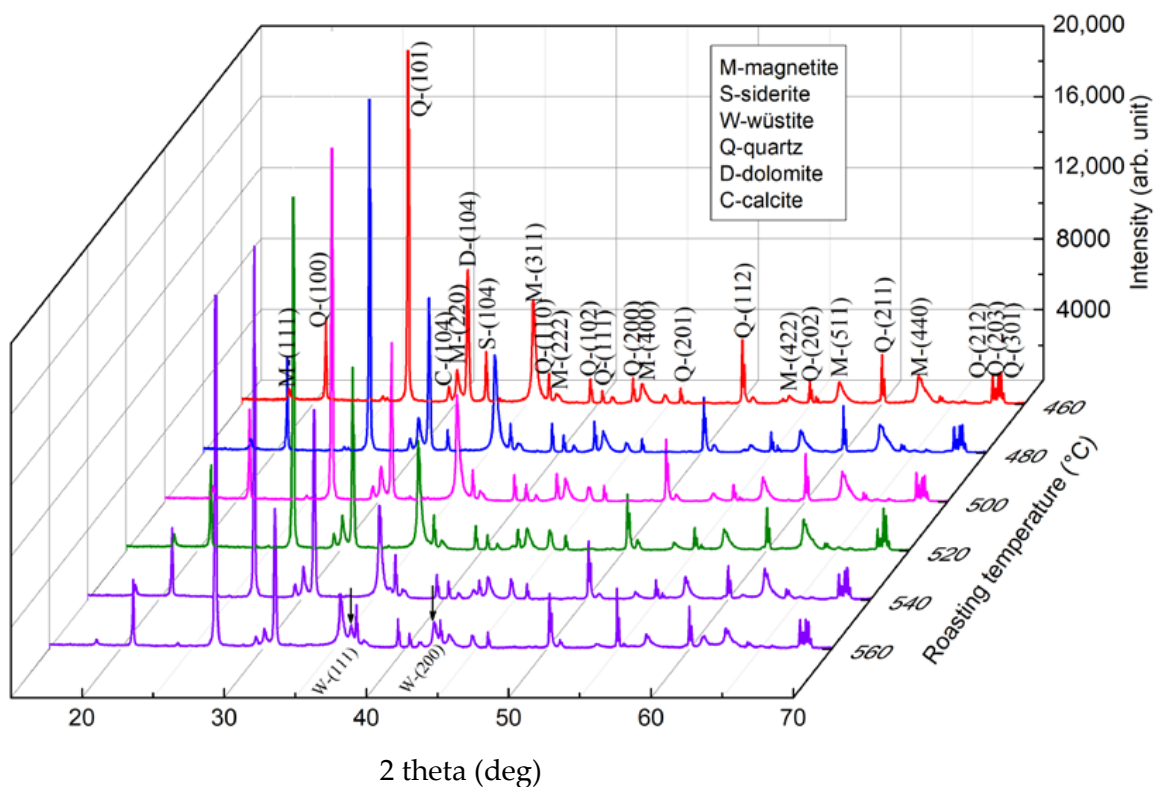
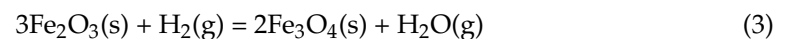
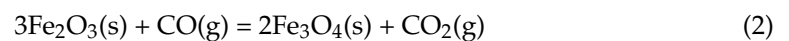
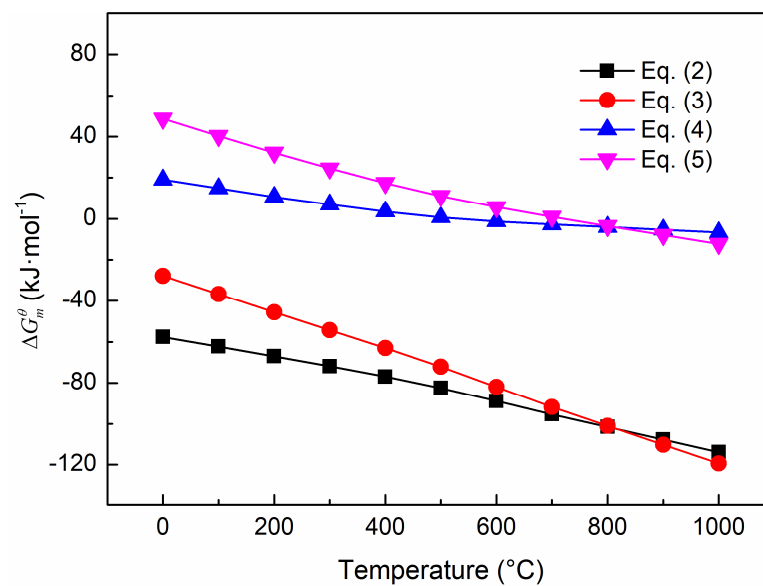


Figure 4. XRD analysis of the roasted products at different roasting temperatures.



**Figure 5.** Thermodynamics analysis of reduction reaction Equations (2)–(5).

### 3.4. Magnetism Properties

To study the magnetism variation in the process, the raw ore, pre-concentration concentrate, roasted ore, and iron concentrate were analysed using a vibrating sample magnetometer and the results are shown in Figure 6. Owing to the increase in the content of ferrimagnetic magnetite, magnetism significantly increased in this process [44]. The saturation magnetization of the raw ore was  $5.69 \text{ A}\cdot\text{m}^2/\text{g}$  because of the existence of a small amount of magnetite. The saturation magnetization increased to  $8.79 \text{ A}\cdot\text{m}^2/\text{g}$  after pre-concentration, which was caused by the removal of coarse gangue minerals. In the suspension magnetization roasting, hematite was reduced to magnetite, which caused the saturation magnetization of roasted ore to increase to  $41.20 \text{ A}\cdot\text{m}^2/\text{g}$ . The saturation magnetization of the iron concentrate significantly increased to  $53.35 \text{ A}\cdot\text{m}^2/\text{g}$  because fine dissemination gangue minerals were liberated and removed in the low-intensity magnetic separation.

### 3.5. Micromorphology Analysis

The micromorphology of roasted products was investigated by using SEM-EDS, and the results are shown in Figure 7. The surface structure of the pre-concentration concentrate (the feed to the suspension magnetization roasting) was relatively intact, dense, and smooth. Some micro-cracks and porous structures appeared on the surface of roasted samples in magnetization roasting. The surface structure of roasted samples was destroyed and showed a honeycomb morphology. The loose and porous structures of samples promoted the diffusion of reducing gas inside the ore, which was conducive to the gas-solid reactions as Equations (2) and (3) in magnetization roasting [31].

### 3.6. Product Property Analysis

#### 3.6.1. Chemical Elemental Analysis

The chemical elemental analyses of magnetic concentrate, pre-concentration tailing, and magnetic tailing are shown in Table 3. It is shown that the Fe and FeO contents of magnetic concentrate were 62.16% and 25.47%, which can be used as an iron concentrate for ironmaking. The main impurity was  $\text{SiO}_2$  and its content was 5.38%. The contents of other impurities MgO,  $\text{Al}_2\text{O}_3$ , and CaO were 1.11%, 1.19%, and 1.88%, respectively. The contents of harmful P and S were 0.036% and 0.052%. The  $\text{SiO}_2$  contents of pre-concentration tailing and magnetic tailing were 81.55% and 79.57%, respectively, which can be used to produce building materials [32,39,40].

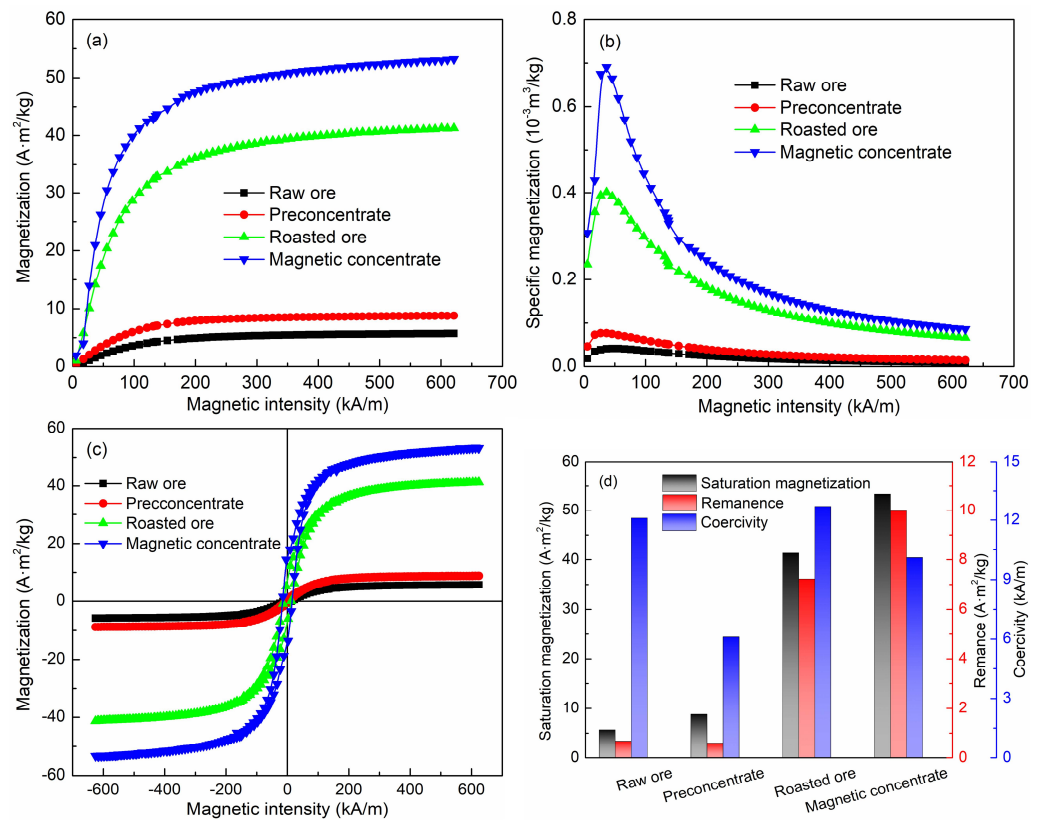


**Figure 6.** Magnetism properties of different products (a) initial magnetization curves; (b) Specific susceptibility curves; (c) hysteresis loops; (d) magnetism parameters.

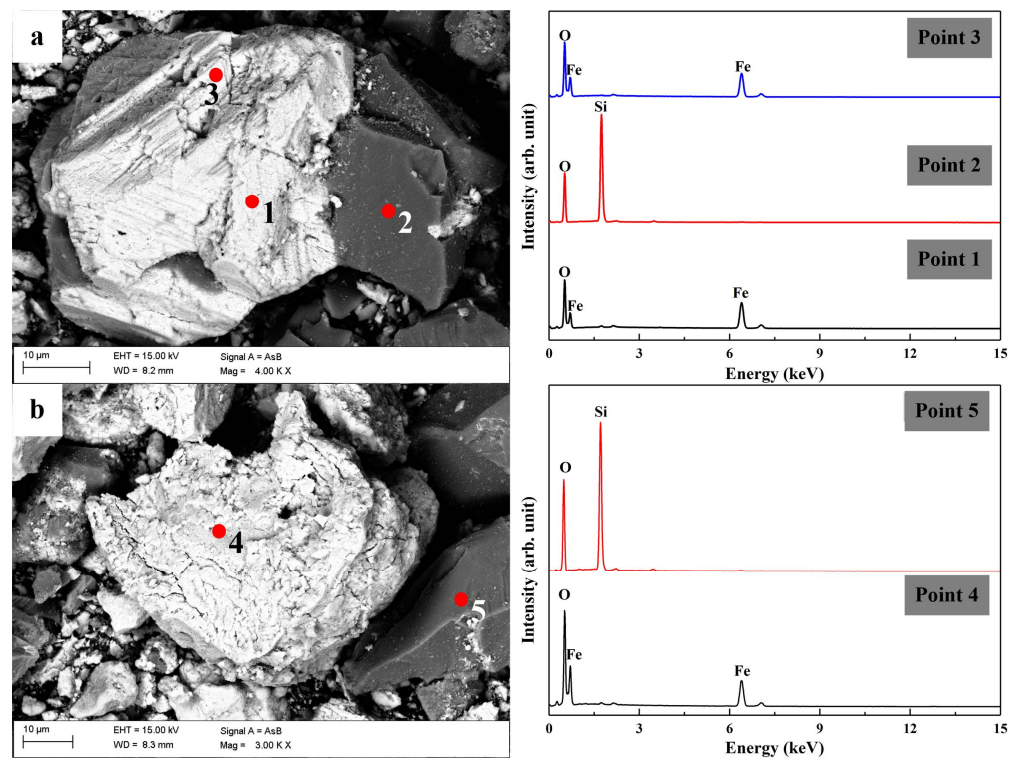


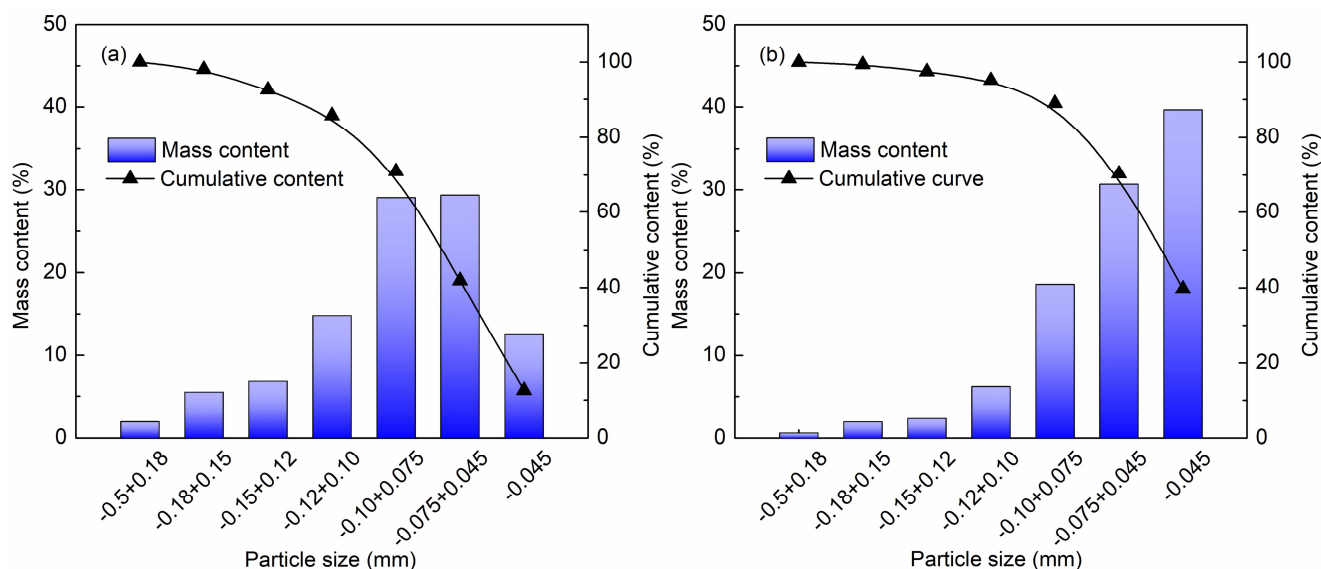
**Figure 7.** Micromorphology analysis of different products (a) pre-concentration concentrate; (b) roasted samples.

**Table 3.** Chemical elemental analysis of different stage products.

Products	Composition and Content (wt.%)							
	Fe	FeO	SiO <sub>2</sub>	Al <sub>2</sub> O <sub>3</sub>	CaO	MgO	S	P
Iron concentrate	62.16	25.47	5.38	1.19	1.88	1.11	0.052	0.036
Pre-concentration tailing	6.70	0.59	81.55	1.72	1.55	0.33	0.032	0.049
Magnetic tailing	4.90	0.85	79.57	2.35	3.07	1.00	0.009	0.055

### 3.6.2. Particle Size Analysis

The particle size analyses of pre-concentration and magnetic tailings were conducted, and the results are shown in Figure 8. Based on the results, the particle size of pre-concentration tailing was coarser than that of magnetic tailing. The particle size of the pre-concentration tailing was 41.87 wt.% below 0.075 mm, and 70.34 wt.% above 0.075 mm of the magnetic tailing. Based on the particle size results, the tailings can be used as fine aggregate and cementitious materials in concrete, cement, and brick making owing to their different particle sizes [32,36,39].

**Figure 8.** Particle size analysis of tailings (a) pre-concentration tailing; (b) magnetic tailing.

## 4. Conclusions

In this study, a combined technology of pre-concentration, suspension magnetization roasting, and low-intensity magnetic separation was presented to utilize low-grade hematite ore resources. The gangue mineral with a yield of 29.01% was effectively removed before suspension magnetization roasting, weakening their influence on the subsequent operation. In suspension magnetization roasting, hematite was transformed into magnetite by the reductant of CO and H<sub>2</sub> mixture. The magnetism significantly strengthened owing to the formation of ferrimagnetic magnetite, and the saturation magnetization of roasted samples was 41.20 A·m<sup>2</sup>/g. The loose and porous structures of roasted samples were conducive to the gas-solid reaction per Equations (2) and (3). Finally, an iron concentrate with a grade of 62.21% and a recovery of 85.72%, a pre-concentration tailing with a SiO<sub>2</sub> grade of 81.55%, and a magnetic tailing with a SiO<sub>2</sub> grade of 79.57% were obtained, which can be used for ironmaking and producing building materials. This has significant implications for the comprehensive utilization of low-grade iron ore.

**Author Contributions:** Conceptualization, X.Z.; methodology, X.Z.; software, Y.Q.; validation, Y.Q.; formal analysis, Y.Q.; investigation, X.Z.; resources, Y.L.; data curation, Y.Q.; writing—original draft preparation, Y.Q.; writing—review and editing, X.Z.; visualization, X.Z.; supervision, Y.H. and Y.L.; project administration, Y.H. and Y.L.; funding acquisition, Y.H. and X.Z. All authors have read and agreed to the published version of the manuscript.

**Funding:** This research was funded by National Natural Science Foundation of China (Nos. 52104249 and 51734005), China Postdoctoral Science Foundation (Grant No. 2021M700726) and Fundamental Research Funds for the Central Universities (N2101034).

**Conflicts of Interest:** The authors declare no conflict of interest.

## References

1. Hu, M.; Pauliuk, S.; Wang, T.; Huppel, G.; van der Voet, E.; Müller, D.B. Iron and steel in Chinese residential buildings: A dynamic analysis. *Resour. Conserv. Recycl.* **2010**, *54*, 591–600. [CrossRef]
2. Yellishetty, M.; Ranjith, P.G.; Tharumarajah, A. Iron ore and steel production trends and material flows in the world: Is this really sustainable? *Resour. Conserv. Recycl.* **2010**, *54*, 1084–1094. [CrossRef]
3. Yellishetty, M.; Mudd, G.M. Substance flow analysis of steel and long term sustainability of iron ore resources in Australia, Brazil, China and India. *J. Clean. Prod.* **2014**, *84*, 400–410. [CrossRef]
4. Hurst, L. Assessing the competitiveness of the supply side response to China's iron ore demand shock. *Resour. Policy* **2015**, *45*, 247–254. [CrossRef]
5. Salisu, A.A.; Adediran, I.A. Assessing the inflation hedging potential of coal and iron ore in Australia. *Resour. Policy* **2019**, *63*, 101410. [CrossRef]
6. Ministry of Natural Resources, PRC. China Mineral Resources. 2019. Available online: [http://www.mnr.gov.cn/sj/sjfw/kc\\_19263/zgkczybg/201910/P020191022538918416752.pdf](http://www.mnr.gov.cn/sj/sjfw/kc_19263/zgkczybg/201910/P020191022538918416752.pdf) (accessed on 1 April 2022).
7. Li, G. The Chinese Iron Ore Deposits and Ore Production. Available online: <https://www.intechopen.com/chapters/61492> (accessed on 1 April 2022).
8. Sun, Y.; Zhu, X.; Han, Y.; Li, Y.; Gao, P. Iron recovery from refractory limonite ore using suspension magnetization roasting: A pilot-scale study. *J. Clean. Prod.* **2020**, *261*, 121221. [CrossRef]
9. Liu, S.; Zhao, Y.; Wang, W.; Wen, S. Beneficiation of a low-grade, hematite-magnetite ore in China. *Min. Metall. Explor.* **2014**, *31*, 136–142. [CrossRef]
10. Zhang, X.; Gu, X.; Han, Y.; Parra-Álvarez, N.; Claremboux, V.; Kawatra, S.K. Flotation of Iron Ores: A Review. *Miner. Process. Extr. Metall. Rev.* **2021**, *42*, 184–212. [CrossRef]
11. Filippov, L.O.; Severov, V.V.; Filippova, I.V. An overview of the beneficiation of iron ores via reverse cationic flotation. *Int. J. Miner. Process.* **2014**, *127*, 62–69. [CrossRef]
12. Liu, W.; Liu, W.; Wang, B.; Duan, H.; Peng, X.; Chen, X.; Zhao, Q. Novel hydroxy polyamine surfactant *N*-(2-hydroxyethyl)-*N*-dodecyl-ethanediamine: Its synthesis and flotation performance study to quartz. *Miner. Eng.* **2019**, *142*, 105894. [CrossRef]
13. He, J.; Zhu, L.; Bu, X.; Liu, C.; Luo, Z.; Yao, Y. Intensification of waste gangue removal from 6–1 mm fine-sized iron ores based on density-based dry vibrated separation and upgrading. *Chem. Eng. Process. Process Intensif.* **2019**, *138*, 27–35. [CrossRef]
14. He, J.; Liu, C.; Hong, P.; Yao, Y.; Luo, Z.; Zhao, L. Mineralogical characterization of the typical coarse iron ore particles and the potential to discharge waste gangue using a dry density-based gravity separation. *Powder Technol.* **2019**, *342*, 348–355. [CrossRef]
15. Lima, R.M.F.; Abreu, F.d.P.V.F. Characterization and concentration by selective flocculation/magnetic separation of iron ore slimes from a dam of Quadrilátero Ferrífero—Brazil. *J. Mater. Res. Technol.* **2020**, *9*, 2021–2027. [CrossRef]
16. Song, S.; Lu, S.; Lopez-Valdivieso, A. Magnetic separation of hematite and limonite fines as hydrophobic flocs from iron ores. *Miner. Eng.* **2002**, *15*, 415–422. [CrossRef]
17. Luo, X.; Wang, Y.; Wen, S.; Ma, M.; Sun, C.; Yin, W.; Ma, Y. Effect of carbonate minerals on quartz flotation behavior under conditions of reverse anionic flotation of iron ores. *Int. J. Miner. Process.* **2016**, *152*, 1–6. [CrossRef]
18. Zhu, Z.; Li, Z.; Yin, W.; Yang, B.; Qu, J.; Zhang, N.; Chen, S.; Yu, Y.; Chang, J.; Liu, L. Snap-in interactions between water droplets and hematite/quartz surfaces with various roughness after conditioning with soluble starch and DDA using a dynamic microbalance. *Miner. Eng.* **2022**, *177*, 107358. [CrossRef]
19. Liu, W.B.; Sun, W.; Liu, W.G.; Dai, S.; Duan, H.; Zhou, S.; Qiu, J. An ion-tolerance collector AESNa for effective flotation of magnesite from dolomite. *Miner. Eng.* **2021**, *170*, 106991. [CrossRef]
20. Quast, K. A review on the characterisation and processing of oolitic iron ores. *Miner. Eng.* **2018**, *126*, 89–100. [CrossRef]
21. Matiolo, E.; Couto, H.J.B.; Lima, N.; Silva, K.; de Freitas, A.S. Improving recovery of iron using column flotation of iron ore slimes. *Miner. Eng.* **2020**, *158*, 106608. [CrossRef]
22. Liu, W.; Peng, X.; Liu, W.; Wang, X.; Zhao, Q.; Wang, B. Effect mechanism of the iso-propanol substituent on amine collectors in the flotation of quartz and magnesite. *Powder Technol.* **2020**, *360*, 1117–1125. [CrossRef]
23. Dong, L.; Tong, X.; Li, X.; Zhou, J.; Wang, S.; Liu, B. Some developments and new insights of environmental problems and deep mining strategy for cleaner production in mines. *J. Clean. Prod.* **2019**, *210*, 1562–1578. [CrossRef]

24. Cui, X.; Geng, Y.; Li, T.; Zhao, R.; Li, X.; Cui, Z. Field application and effect evaluation of different iron tailings soil utilization technologies. *Resour. Conserv. Recycl.* **2021**, *173*, 105746. [[CrossRef](#)]
25. Zhang, Y.; Tang, Z.; Shirokoff, J. Study on Flotability and Surface Oxidation of Sulfide Minerals from the Tailing of an Iron-Copper Mine Using Electron Probe Microanalyzer. *Miner. Process. Extr. Metall. Rev.* **2021**, *42*, 213–221. [[CrossRef](#)]
26. Uwadiae, G.G.O.O. Magnetizing Reduction of Iron Ores. *Miner. Process. Extr. Metall. Rev.* **1992**, *11*, 1–19. [[CrossRef](#)]
27. Yu, J.; Han, Y.; Li, Y.; Gao, P.; Li, W. Mechanism and Kinetics of the Reduction of Hematite to Magnetite with CO–CO<sub>2</sub> in a Micro-Fluidized Bed. *Minerals* **2017**, *7*, 209. [[CrossRef](#)]
28. Yu, J.; Han, Y.; Li, Y.; Gao, P. Recent Advances in Magnetization Roasting of Refractory Iron Ores: A Technological Review in the Past Decade. *Miner. Process. Extr. Metall. Rev.* **2019**, *41*, 349–359. [[CrossRef](#)]
29. Roy, S.K.; Nayak, D.; Rath, S.S. A review on the enrichment of iron values of low-grade Iron ore resources using reduction roasting-magnetic separation. *Powder Technol.* **2020**, *367*, 796–808. [[CrossRef](#)]
30. Jin, J.; Zhu, X.; Li, P.; Li, Y.; Han, Y. Clean Utilization of Limonite Ore by Suspension Magnetization Roasting Technology. *Minerals* **2022**, *12*, 260. [[CrossRef](#)]
31. Tang, Z.; Zhang, Q.; Sun, Y.; Gao, P.; Han, Y. Pilot-scale extraction of iron from flotation tailings via suspension magnetization roasting in a mixture of CO and H<sub>2</sub> followed by magnetic separation. *Resour. Conserv. Recycl.* **2021**, *172*, 105680. [[CrossRef](#)]
32. Rana, A.; Kalla, P.; Verma, H.K.; Mohnot, J.K. Recycling of dimensional stone waste in concrete: A review. *J. Clean. Prod.* **2016**, *135*, 312–331. [[CrossRef](#)]
33. Zhai, W.; Ding, J.; An, X.; Wang, Z. An optimization model of sand and gravel mining quantity considering healthy ecosystem in Yangtze River, China. *J. Clean. Prod.* **2020**, *242*, 118385. [[CrossRef](#)]
34. Gavriletea, M.D. Environmental Impacts of Sand Exploitation. Analysis of Sand Market. *Sustainability* **2017**, *9*, 1118. [[CrossRef](#)]
35. Patil, A.Y.; Banapurmath, N.R.; Shivangi, U.S. Feasibility study of epoxy coated Poly Lactic Acid as a sustainable replacement for river sand. *J. Clean. Prod.* **2020**, *267*, 121750. [[CrossRef](#)]
36. Ren, Z.; Jiang, M.; Chen, D.; Yu, Y.; Li, F.; Xu, M.; Bringezu, S.; Zhu, B. Stocks and flows of sand, gravel, and crushed stone in China (1978–2018): Evidence of the peaking and structural transformation of supply and demand. *Resour. Conserv. Recycl.* **2022**, *180*, 106173. [[CrossRef](#)]
37. Cao, Y.; Wang, Y.; Zhang, Z.; Wang, H. Recycled sand from sandstone waste: A new source of high-quality fine aggregate. *Resour. Conserv. Recycl.* **2022**, *179*, 106116. [[CrossRef](#)]
38. Liu, W.B.; Peng, X.Y.; Liu, W.G.; Zhang, N.; Wang, X.Y. A cost-effective approach to recycle serpentine tailings: Destruction of stable layered structure and solvent displacement crystallization. *Int. J. Min. Sci. Technol.* **2022**, *in press*. [[CrossRef](#)]
39. Yellishetty, M.; Karpe, V.; Reddy, E.H.; Subhash, K.N.; Ranjith, P.G. Reuse of iron ore mineral wastes in civil engineering constructions: A case study. *Resour. Conserv. Recycl.* **2008**, *52*, 1283–1289. [[CrossRef](#)]
40. Xu, W.; Wen, X.; Wei, J.; Xu, P.; Zhang, B.; Yu, Q.; Ma, H. Feasibility of kaolin tailing sand to be as an environmentally friendly alternative to river sand in construction applications. *J. Clean. Prod.* **2018**, *205*, 1114–1126. [[CrossRef](#)]
41. Vargas, F.; Lopez, M.; Rigamonti, L. Environmental impacts evaluation of treated copper tailings as supplementary cementitious materials. *Resour. Conserv. Recycl.* **2020**, *160*, 104890. [[CrossRef](#)]
42. Loginova, E.; Schollbach, K.; Proskurnin, M.; Brouwers, H.J.H. Municipal solid waste incineration bottom ash fines: Transformation into a minor additional constituent for cements. *Resour. Conserv. Recycl.* **2021**, *166*, 105354. [[CrossRef](#)]
43. Zhang, X.; Han, Y.; Sun, Y.; Li, Y. Innovative utilization of refractory iron ore via suspension magnetization roasting: A pilot-scale study. *Powder Technol.* **2019**, *352*, 16–24. [[CrossRef](#)]
44. Zhu, X.; Han, Y.; Sun, Y.; Gao, P.; Li, Y. Thermal Decomposition of Siderite Ore in Different Flowing Atmospheres: Phase Transformation and Magnetism. *Miner. Process. Extr. Met. Rev.* **2022**, 1–8. [[CrossRef](#)]